Acta Biomaterialia xxx (2016) xxx–xxx

Contents lists available at ScienceDirect

Acta Biomaterialia

journal homepage: www.elsevier.com/locate/actabiomat

Scaffold-free parathyroid tissue engineering using tonsil-derived mesenchymal stem cells

Yoon Shin Park [a,b,c,1], Ji-Young Hwang [d,1], Yesl Jun [d,e], Yoon Mi Jin [a,b], Gyungah Kim [a,b], Ha Yeong Kim [a,b], Han Su Kim [b,f], Sang-Hoon Lee [d,e,g,*], Inho Jo [a,b,*]

[a] Department of Molecular Medicine, School of Medicine, Ewha Womans University, Seoul 158-710, Republic of Korea
[b] Ewha Tonsil-derived mesenchymal Stem cells Research Center (ETSRC), School of Medicine, Ewha Womans University, Seoul 158-710, Republic of Korea
[c] School of Life Science, College of Natural Sciences, Chungbuk National University, Cheongju 361-763, Republic of Korea
[d] Department of Biomedical Engineering, College of Health Science, Korea University, Seoul 136-713, Republic of Korea
[e] KU-KIST Graduate School of Converging Science & Technology, Korea University, Seoul 136-713, Republic of Korea
[f] Department of Otorhinolaryngology – Head & Neck Surgery, School of Medicine, Ewha Womans University, Seoul 158-710, Republic of Korea
[g] Department of Bio-convergence Engineering, College of Health Science, Korea University, Seoul 136-713, Republic of Korea

ARTICLE INFO

Article history:
Received 28 October 2015
Received in revised form 27 February 2016
Accepted 1 March 2016
Available online xxxx

Keywords:
Tonsil-derived mesenchymal stem cells
Spheroid
Parathyroid hormone
Hypoparathyroidism
N-cadherin

ABSTRACT

To restore damaged parathyroid function, parathyroid tissue engineering is the best option. Previously, we reported that differentiated tonsil-derived mesenchymal stem cells (dTMSC) restore *in vivo* parathyroid function, but only if they are embedded in a scaffold. Because of the limited biocompatibility of Matrigel, however, here we developed a more clinically applicable, scaffold-free parathyroid regeneration system. Scaffold-free dTMSC spheroids were engineered in concave microwell plates made of polydimethylsiloxane in control culture medium for the first 7 days and differentiation medium (containing activin A and sonic hedgehog) for next 7 days. The size of dTMSC spheroids showed a gradual and significant decrease up to day 5, whereafter it decreased much less. Cells in dTMSC spheroids were highly viable (>80%). They expressed high levels of intact parathyroid hormone (iPTH), the parathyroid secretory protein 1, and cell adhesion molecule, N-cadherin. Furthermore, dTMSC spheroids-implanted parathyroidectomized (PTX) rats revealed higher survival rates (50%) over a 3-month period with physiological levels of both serum iPTH (57.7–128.2 pg/mL) and ionized calcium (0.70–1.15 mmol/L), compared with PTX rats treated with either vehicle or undifferentiated TMSC spheroids. This is the first report of a scaffold-free, human stem cell-based parathyroid tissue engineering and represents a more clinically feasible strategy for hypoparathyroidism treatment than those requiring scaffolds.

Statement of Significance

Herein, we have for the first time developed a scaffold-free parathyroid tissue spheroids using differentiated tonsil-derived mesenchymal stem cells (dTMSC) to restore *in vivo* parathyroid cell functions. This new strategy is effective, even for long periods (3 months), and is thus likely to be more feasible in clinic for hypoparathyroidism treatment. Development of TMSC spheroids may also provide a convenient and efficient scaffold-free platform for researchers investigating conditions involving abnormal calcium homeostasis, such as osteoporosis.

1. Introduction

Hypoparathyroidism mainly occurs when parathyroid glands fail to secrete sufficient parathyroid hormone (PTH) as a largely unavoidable consequence of parathyroidectomy (PTX) followed by thyroidectomy. Since PTH plays a pivotal role in calcium homeostasis in the body [1,2], low PTH production and secretion leads to a lack of calcium in blood and bones [3]. Severe and chronic hypocalcemia can be fatal.

* Corresponding authors at: Department of Bio-convergence Engineering, College of Health Science, Korea University, Seoul 136-713, Republic of Korea (S.-H. Lee). Department of Molecular Medicine, School of Medicine, Ewha Womans University, Seoul 158-710, Republic of Korea (I. Jo).
E-mail addresses: dbiomed@korea.ac.kr (S.-H. Lee), inhojo@ewha.ac.kr (I. Jo).
[1] These authors contributed equally to this work.

http://dx.doi.org/10.1016/j.actbio.2016.03.003
1742-7061/

Several different methods have been used clinically in the treatment of hypoparathyroidism. These include 1) autografting of parathyroid tissues discarded from patients during surgery, an approach associated with uncertainty regarding whether or for how long the graft tissue will survive in the body; 2) daily intake of multiple mega-doses of calcium (1–9 g/day every 6 h) and vitamin D (1.25–5 mg/day) for a remarkably long time, which can provoke hypercalciuria, resulting in kidney problems and vitamin toxicity; and 3) daily injection of the synthetic PTH, teriparatide (brand name, Forteo®), but a maximum of ~2 years is recommended to avoid side effects. At present, the combination of autografting of parathyroid tissues together with multiple high doses of vitamin D and calcium is the most common therapeutic approach [4]. These limitations highlight the need for the development of new therapies, such as direct replacement of functional parathyroid cells without the need for multiple high doses of vitamin D and calcium. In this context, the use of stem cells has recently received considerable attention because of its therapeutic potential for use in tissue engineering and clinical applications [5]. It was previously reported that human embryonic stem cells (hESC) [6] and transdifferentiated thymic stromal cells [7] could be used for the *in vitro* regeneration of parathyroid-like cells. However, these cells have critical limitations for clinical use, including ethical issues associated with the use of hESC and the considerably long time ($\geqslant$10 weeks) required for transdifferentiation of thymic stromal cells into PTH-secreting parathyroid-like cells. To overcome these limitations, we recently introduced human tonsil-derived mesenchymal stem cells (TMSC) for *in vivo* parathyroid tissue regeneration [8]. However, the therapeutic potential of TMSC against hypoparathyroidism in this previous study was limited; differentiated TMSC (dTMSC), but not undifferentiated, control TMSC (cTMSC), resembled parathyroid cells *in vitro* and, more importantly, they only restored parathyroid functions *in vivo* when embedded in a scaffold, Matrigel. Problems associated with scaffolds themselves have been a recurring clinical issue in tissue regeneration.

Tissue regeneration using scaffold-free conditions has recently been highly recommended for safe and long-term clinical applications [9,10]. To this end, we previously established a novel method for three-dimensional (3D) spheroidal culture of various types of cells to manufacture organoids for tissue regeneration [11,12]. For example, rat hepatocytes engineered in a 3D spheroid system have been previously reported to exhibit greater advantages for liver regeneration [12–14]. Another example is the enhanced viability and *in vivo* function of spheroidal cultures of adipose tissue-derived MSC (AD-MSC) and pancreatic islets in an animal model of type I diabetes mellitus [15,16]. Although detailed underlying mechanisms have not yet been elucidated, cells within spheroids appear to exert concerted effects on one another.

On the basis of our previous studies, we here investigated whether a scaffold-free engineering of 3D organoids using dTMSC can surmount requirements for a Matrigel scaffold to restore *in vivo* parathyroid cell functions. Our current results clearly showed that implantation with self-assembled dTMSC spheroids significantly increases survival rates and the levels of serum intact PTH (iPTH) and ionized calcium (iCa^{2+}) in a PTX rat model, suggesting the greater likelihood of applying a scaffold-free system to parathyroid regeneration in a clinical setting.

2. Materials and methods

2.1. Isolation and culture of TMSC

TMSC were isolated and cultured as previously described [8,17]. Briefly, a total of five patients less than 10 years of age undergoing tonsillectomy (3 boys and 2 girls; mean age, 6.2 years) were recruited at random from consecutive patients presenting between April 2012 and December 2012 at the Department of Otorhinolaryngology–Head and Neck Surgery, Ewha Womans University Medical Center (EWUMC, Seoul, Republic of Korea). Informed written consent was obtained from legal guardians of all patients participating in this study, and the study protocol was approved by the institutional review board of EWUMC (IRB No. ECT-11-53-02).

Isolated tonsillar tissue was chopped and digested with collagenase type I (Invitrogen Corp., Carlsbad, CA, USA) and DNase (Sigma–Aldrich, St Louis, MO, USA) for 30 min at 37 °C. Digested tissue was filtered through a wire mesh and washed with RPMI-1640 medium containing normal human serum, after which adherent mononuclear cells were obtained by Ficoll-Paque (GE Healthcare, Little Chalfont, UK) density gradient centrifugation. Cells were then cultured in high-glucose (4500 mg/L) Dulbecco's Modified Eagle Medium (DMEM-HG; Welgene Inc., Gyeongsan, Republic of Korea) containing 10% fetal bovine serum (FBS; Invitrogen). After 48 h, non-adherent cells were discarded and adherent mononuclear cells (hereafter called TMSC) were cultured. All TMSC used in this study were between passage 3 and 9.

2.2. Differentiation into parathyroid-like cells

TMSC were differentiated into parathyroid-like cells using the modified Bingham protocol [18], as previously described [8,17]. Briefly, cells were incubated in 3D culture conditions in the absence or presence of differentiation medium for the indicated times (0, 7, and 14 days) (Fig. 1). Differentiation medium contained activin A (100 ng/mL, R&D Systems Inc., Minneapolis, MN, USA) and soluble sonic hedgehog (Shh; 100 ng/mL, R&D Systems Inc.) and was changed every other day.

2.3. Fabrication of concave molds

Polydimethylsiloxane (PDMS; Dow Corning, Midland, MI, USA)-based concave molds were fabricated using soft lithography techniques with a PDMS membrane and SU-8 mold plates, as previously described [19,20]. Briefly, vacuum pressure was applied to an acrylic chamber to deflect the SU-8 prepolymer on the PDMS membrane to form convex SU-8 structures. The concave PDMS microwell structure was fabricated using the SU-8 plate as a master mold. In this study, we used concave microwell molds 500 μm in diameter, 250 μm in depth and 500 μm apart at a density of 100 wells/cm^2 (StemFIT 3D; MicroFIT, Seonnam, Republic of Korea).

2.4. Formation and culture of TMSC spheroids

All microwell plates were pre-coated with 3% (w/v) bovine serum albumin (BSA, Sigma–Aldrich) before use to minimize cell attachment. After TMSC were dispersed into a single-cell

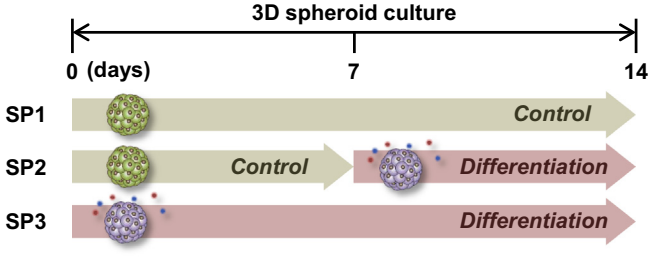

Fig. 1. Three experimental groups for constructing TMSC spheroids. TMSC were cultured in the absence or presence of differentiation culture medium for the indicated times under 3D condition. TMSC spheroids are classified into three groups as follows: SP1 (TMSC in control culture medium for all 14 days); SP2 (TMSC in control medium for the first 7 days, followed by differentiation medium for the second 7 days); SP3 (TMSC in differentiation medium for all 14 days).

Please cite this article in press as: Y.S. Park et al., Scaffold-free parathyroid tissue engineering using tonsil-derived mesenchymal stem cells, Acta Biomater. (2016), http://dx.doi.org/10.1016/j.actbio.2016.03.003

suspension by trypsin digestion, a total of 2×10^5 cells were gently seeded at 200 μL per mold. Under these conditions, most cells were evenly docked into each well. Five minutes after TMSC seeding, a gentle flow of culture medium was applied to remove cells that had not docked within microwells. Docked TMSC were then cultured without or with differentiation medium for the indicated times (Fig. 1) and replenished with new culture medium every other day. TMSC spheroids were constructed and cultured as follows (Fig. 1); 1) spheroids 1 (SP1), cultured in control culture medium for all 14 days; 2) SP2, cultured in control medium for the first 7 days and in differentiation medium for the next 7 days; 3) SP3, cultured in differentiation medium for all 14 days.

2.5. Measurement of TMSC spheroid morphology and size

TMSC segregation, aggregation, and spheroid formation were observed daily under a microscope (EVOS Cell Imaging Systems; Life Technologies, Carlsbad, CA, USA). TMSC spheroids were fixed with 2.5% glutaraldehyde in deionized water for 1 h and gently washed 3–5 times with deionized water. For secondary fixation, TMSC spheroids were immersed in 1% osmium tetroxide (Sigma–Aldrich) in deionized water for 1 h. Fixed spheroids were then dehydrated with a graded ethanol series (25%, 50%, 75%, 95%, and 100%), immersed three times in tert-butyl alcohol for 30 min at room temperature, and frozen at -70 °C. The tert-butyl alcohol was then evaporated by freeze-drying, after which spheroids were mounted onto a specimen stub with graphite paste and coated with palladium alloy. The surface morphology of spheroids was observed under a scanning electron microscope (SEM; JEOL Ltd., Tokyo, Japan), and their size distributions were analyzed using Image J (NIH, Bethesda, MD, USA).

2.6. Cell viability assay

The viability of cells in TMSC spheroids was evaluated using Live/Dead assay reagents (50 mM calcein-acetoxymethyl ester and 25 mg/mL ethidium homodimer-1; Invitrogen) in culture medium for 40 min at 37 °C. The labeled cells were subsequently observed and images were acquired by confocal microscopy (Olympus, Tokyo, Japan).

2.7. Immunofluorescence analysis

TMSC spheroids were fixed with 4% (w/v) paraformaldehyde at 4 °C for 60 min, washed gently three times with phosphate buffered saline (PBS), and immersed overnight in 20% sucrose in PBS at 4 °C. Samples were embedded in optimal cutting temperature (OCT) compound (Sakura Finetek, Torrance, CA, USA) and kept as frozen blocks at −80 °C. Frozen samples were cut into 10-μm-thick sections using a cryostat and placed on HistoBond adhesive microscope glass slides (Marienfeld-Superior, Lauda-Koenigshofen, Germany). In a separate experiment, TMSC spheroids-implanted skin tissues isolated from PTX rats were also examined after embedding in a paraffin block. Paraffin-embedded skin tissues were cut into 10–μm-thick sections using a rotary microtome (LEICA RM 2135, LEICA Biosystems, Heidelberg, Germany) and placed on HistoBond adhesive microscope glass slides. After de-paraffinization, glass slides were air-dried for 30 min and rinsed several times with PBS. For immunofluorescence assays, all samples were blocked by incubating with a 1% BSA solution for 1 h, and then were incubated with primary anti-PTH rabbit monoclonal antibody (1:100; AbFrontier, Seoul, Republic of Korea), anti-CHGA mouse polyclonal antibody (1:100; AbFrontier), anti-N-cadherin mouse polyclonal antibody (1:100; BD Biosciences, San Jose, CA, USA), anti-CD31 rabbit polyclonal antibody (1:100; Abcam, Cambridge, UK), or anti-GCM2 rabbit monoclonal antibody (1:100; Santa Cruz Biotechnology, Dallas, TX, USA). CHGA and GCM2 stand for chromogranin A, the parathyroid secretory protein 1 and glial cells missing homolog 2, respectively. Samples were rinsed with PBS and incubated at room temperature for 60 min with Alexa Fluor 488-conjugated anti-rabbit or -mouse, or Alexa Fluor 594-conjugated anti-mouse secondary antibodies (Life Technologies), as appropriate, followed by counterstaining nuclei with 4′,6-diamidino-2-phenylindole (DAPI; Life Technologies). Images were obtained using a laser-scanning confocal fluorescence microscope (Olympus, Tokyo, Japan), and fluorescence intensities of green or red versus blue were normalized using the SP1 group as a control.

2.8. Animals and development of PTX rats

Male Sprague-Dawley (SD) rats weighing ~200 g (Orient Bio, Seoul, Republic of Korea) were housed under a 12-h light/dark cycle and provided *ad libitum* access to a standard AIN-93G diet (calcium concentration = 5 g/kg body weight, 0.5%) before PTX. PTX was accomplished as described previously [8,21]. All experimental procedures were reviewed and approved by the ethics committee for animal research of EWUMC (based on the policies of the Institutional Animal Care and Use Committee). Briefly, rats were photosensitized by intraperitoneal injection of 5-aminolevulinic acid (5-ALA; 250 mg/kg, Sigma–Aldrich) and were kept under subdued light for 2 h. Thereafter, rats were anesthetized with Zoletil (Virbac, Seoul, Republic of Korea)/xylazine (Rompun) (Bayer Korea, Seoul, Republic of Korea) (1:1 mixture, 0.1 mL/100 g body weight). The skin on the anterior part of the neck was longitudinally incised, and the trachea and thyroid were exposed. Parathyroid glands were detected under a xenon light source (405 nm) based on the presence of red fluorescence anterolaterally to the thyroid gland, and bilateral parathyroid glands were surgically removed. After surgery, the incision was closed with nylon suture (No. 5.0) and treated with Betadine solution (5% Sterile Ophthalmic Prep Solution; Woodstock, IL, USA) to prevent infection of the wound area. During the experiment, rats whose body weights dropped to less than 80% of their initial weights were euthanized by the CO_2 inhalation method, according to safety and animal experiment guidelines.

2.9. In vivo experimental design

Male SD rats (n = 40) were randomly allocated into five groups (n = 5 per each sham group, n = 10 per each SP1, SP2 and PBS group): 1) Sham, rats with sham operation and without TMSC spheroid implantation; 2) PTX-PBS, PTX rats injected with PBS, 3) PTX-SP1, PTX rats with SP1 implantation; and 4) PTX-SP2, PTX rats with SP2 implantation. Rats in the sham group were then fed a normal standard chow diet (containing 0.5% calcium) or calcium-free diet. All remaining PTX groups were fed a calcium-free diet. Rats in PTX-PBS group received daily intraperitoneal injections of PBS only. Among the three types of TMSC spheroids, only two—SP1 (cTMSC) and SP2 (dTMSC) spheroids—were used for implantation into PTX rats. These experimental groups (PTX-SP1 and PTX-SP2, respectively) received a single subcutaneous injection of the corresponding spheroids. Each group received 1×10^3 spheroids, each containing ~1000 cells, for a total of ~10^6 cells/injection. All animals were monitored for 3 months.

2.10. Assessment of iPTH and iCa^{2+}

Whole blood was collected by jugular vein puncture and analyzed for iPTH and iCa^{2+} concentrations before surgery (day 0) and 1, 3, 7, 14, 21 and 28 days, and 2 and 3 months after implantation, after which serum was separated by centrifugation and stored at −20 °C until use. Serum iPTH was measured by electrochemical

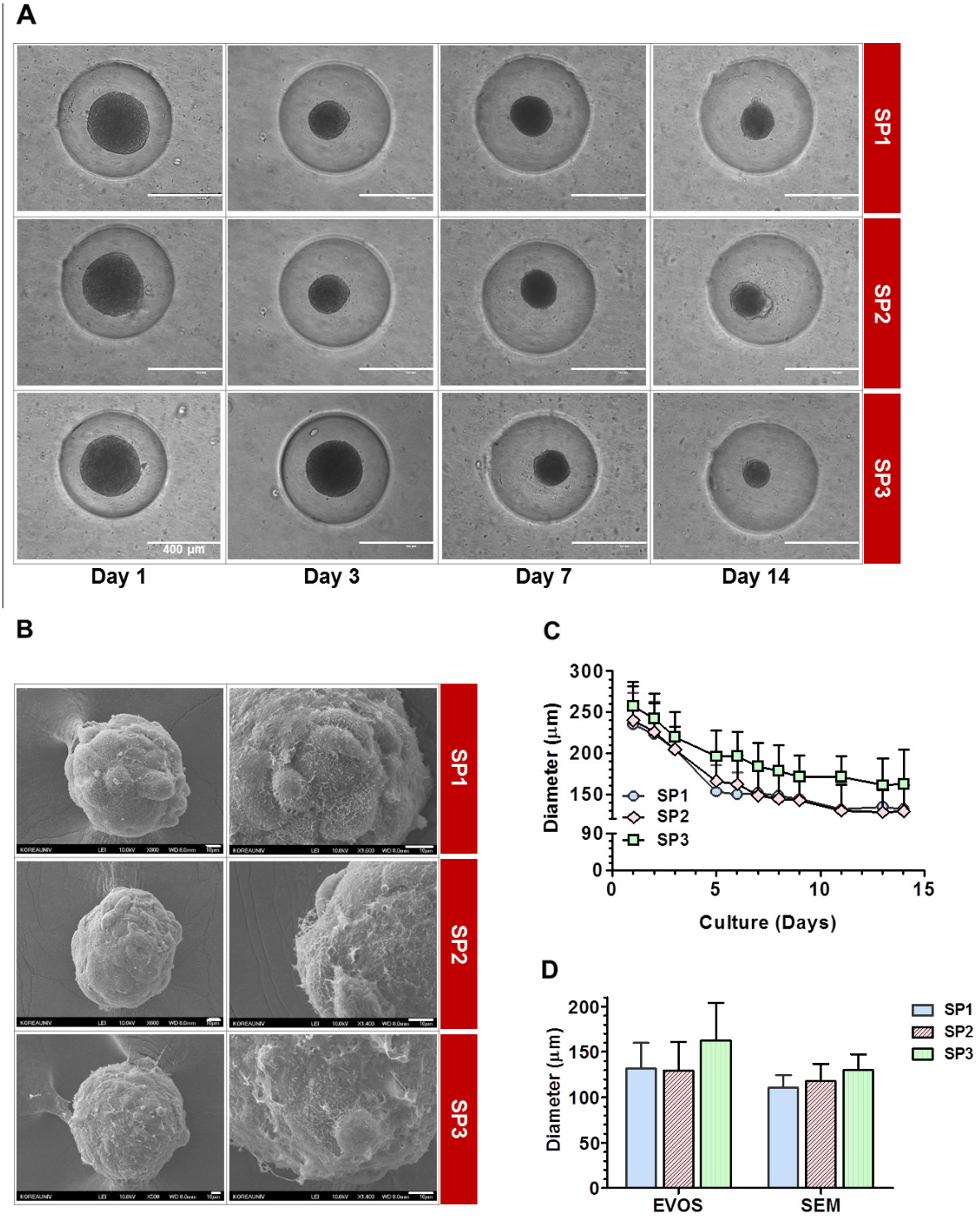

Fig. 2. Characteristics of TMSC spheroids EVOS cell images (A) and SEM images (B) of TMSC spheroids on concave microwells. Scale bars: 400 μm (EVOS) and 10 μm (SEM). (C) Measurement of spheroid sizes based on EVOS cell imaging at different culture times and (D) by EVOS and SEM imaging on day 21. Data were analyzed using one-way ANOVA and are shown as means ± S.D. (n = 52 for EVOS and n = 31–40 for SEM).

luminescence immune assay (ECLIA) using an ELecsys PTH kit (Roche, Basel, Switzerland). Serum iCa^{2+} levels were analyzed using a Ciba-Corning 634 ISE Ca^{2+}/pH analyzer (Ciba-Corning, Essex, UK).

2.11. Statistical analysis

All experiments were repeated at least three times and data are presented as means ± standard deviations (S.D.). Statistical analyses were performed using SPSS ver. 21 (SPSS Inc., Chicago, IL, USA). The statistical significance of differences was determined using Student's *t*-test for paired data and one-way analysis of variance (ANOVA) with post hoc Tukey's honestly significant difference (HSD) test for more than two points. The level of significance was represented as $P < 0.05$ in *t*-test. Different letters indicate significant differences among experimental groups in ANOVA.

Please cite this article in press as: Y.S. Park et al., Scaffold-free parathyroid tissue engineering using tonsil-derived mesenchymal stem cells, Acta Biomater. (2016), http://dx.doi.org/10.1016/j.actbio.2016.03.003

3. Results

3.1. Size of TMSC spheroids

In order to manufacture effective 3D spheroids, a total of 2×10^5 individual TMSC in the absence or presence of differentiation medium were seeded on a 100-microwell concave mold made of PDMS. After washing undocked TMSC, the final number of individual TMSC was estimated to be ~1000 cells/well. Spheroid structures of TMSC were readily detected 1 day after seeding; the diameters of SP1, SP2 and SP3 aggregates at day 1 were 235.3 ± 38.5, 240.2 ± 41.9 and 257.5 ± 29.9 μm, respectively (Fig. 2A and B). Although the sizes of the first two SPs, SP1 and SP2, appeared smaller than that of SP3, they were not statistically different. With time in culture, the sizes of spheroids gradually and significantly decreased up to day 5; the diameters of SP1, SP2 and SP3 were 152.9 ± 33.1, 166.1 ± 32.7 and 195.9 ± 31.8 μm, respectively. However, after day 5, their sizes decreased much less; the corresponding values at day 14 were 131.6 ± 28.4, 129.2 ± 31.6 and 162.4 ± 41.8 μm. As shown in Fig. 2D, SEM revealed that the sizes of TMSC spheroids in group SP1, SP2 and SP3 at day 14 were 110.4 ± 14.0, 117.7 ± 19.2 and 129.9 ± 17.4 μm, respectively (Fig. 2D). The smaller sizes measured by SEM compared with the EVOS cell imaging system likely reflect the dehydration process required for SEM (Fig. 2C and D). All these data suggest that the sizes among three SP groups were not statistically different.

3.2. Viability and morphology in TMSC spheroids

Viability of cells in the three different TMSC spheroids was quantitatively assessed at day 14 by fluorescence microscopy using a Live/Dead assay (Fig. 3A–C), which shows live and dead cells with green and red fluorescence, respectively. The rank order of cell viability for SP groups was SP1 (84.1% ± 3.3%), SP2 (82.4% ± 4.2%) and SP3 (75.3% ± 4.1%) (Fig. 3D). Although there was no significant difference in cell viability between SP1 and SP2 groups, viability was significantly lower in SP3. Therefore, SP3 group was not used in subsequent *in vivo* experiments unless indicated otherwise.

3.3. Expression of parathyroid cell markers in TMSC spheroids

Expression of the parathyroid cell protein markers, PTH and CHGA, in TMSC spheroids was examined using immunofluorescence analysis. As expected, low (basal) expression of PTH and CHGA, either on the surface (Fig. 4A) or in the center (Fig. 4B) of spheroids, was found in the SP1 group, whereas both PTH and CHGA were expressed at significantly higher levels in other two SP groups, after normalization of fluorescence intensities to nuclear fluorescence. PTH expression on both the surface and center of spheroids was significantly higher in SP2 than in SP1 (2.91 ± 0.29-fold and 3.59 ± 0.34-fold, respectively); CHGA expression was similarly higher on the surface (4.77 ± 0.53-fold) and in the center (4.06 ± 0.61-fold) of SP2 compared with SP1 (Fig. 4C and D). On the basis of these data, SP2 was used as the representative dTMSC spheroid group in *in vivo* animal experiments; SP1 was used as a control. It should also be noted that the minimal differentiation condition used for the SP2 group is more cost-effective.

3.4. Improved survival in PTX rats implanted with TMSC spheroids

We first evaluated the survival rates of rats in the various experimental groups. All rats in the sham group survived the entire experimental period (3 months) (Fig. 5A). As expected, survival was the lowest in PTX-PBS rats, with 40% surviving to day 2, and none surviving beyond day 8. However, 60% of PTX-SP2 rats survived for 2 months and 50% survived for 3 months, although

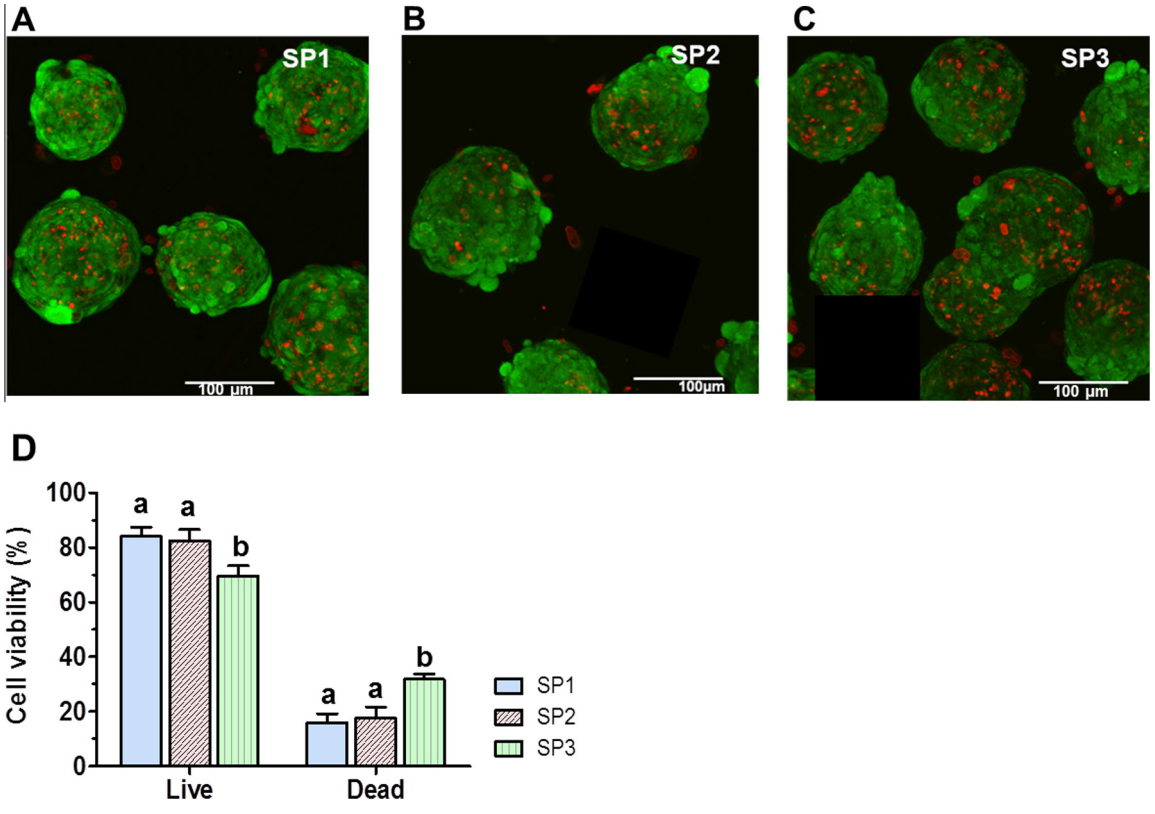

Fig. 3. Cell viability analysis of TMSC spheroids. Staining of (A) SP1, (B) SP2, and (C) SP3 for live cells (green) and dead cells (red). Scale bars: 100 μm. (E) Quantitative analysis of fluorescence intensities by Image J. Data were analyzed using one-way ANOVA and are expressed as means ± S.D. (n = 3–5). Different letters indicate significant differences among experimental groups ($P < 0.05$). (For interpretation of the references to color in this figure legend, the reader is referred to the web version of this article.)

Please cite this article in press as: Y.S. Park et al., Scaffold-free parathyroid tissue engineering using tonsil-derived mesenchymal stem cells, Acta Biomater. (2016), http://dx.doi.org/10.1016/j.actbio.2016.03.003

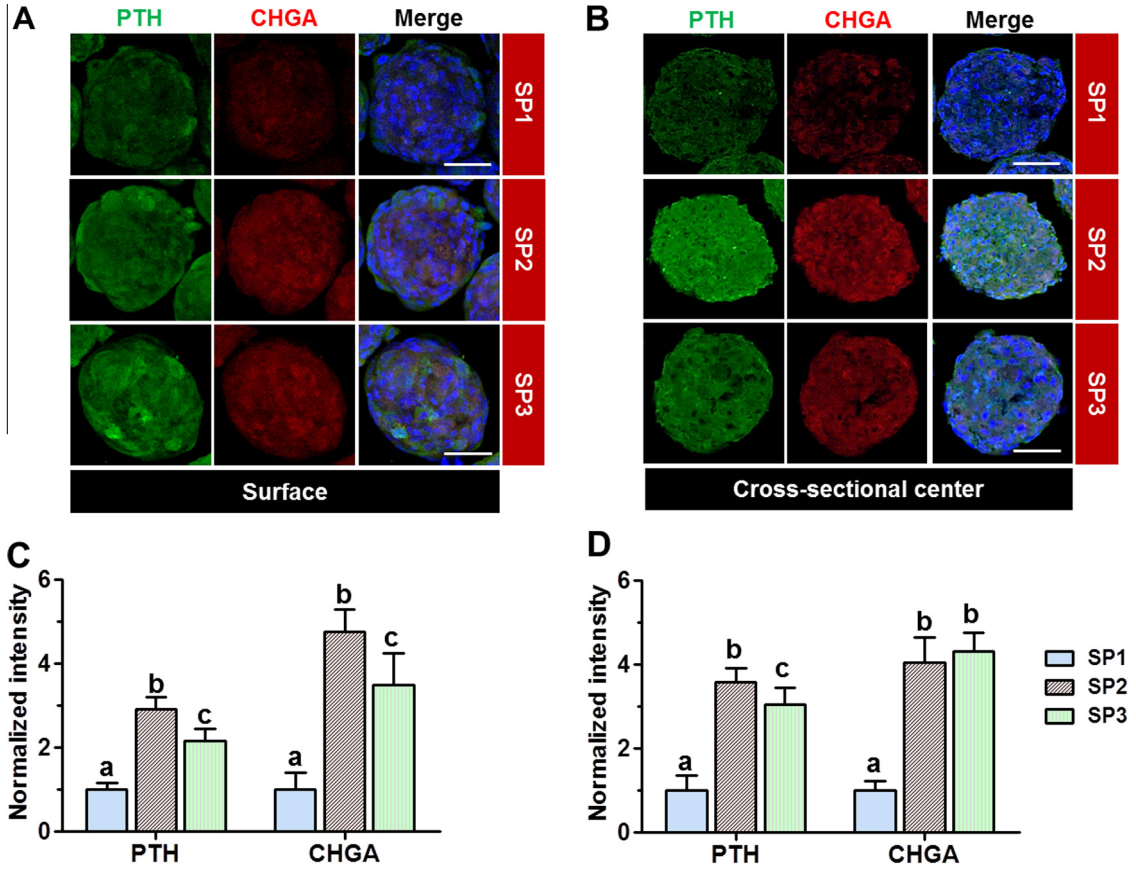

Fig. 4. Immunofluorescence analysis of TMSC spheroids. (A, B) Representative images of each experimental group showing immunofluorescence detection of PTH (green) and CHGA (red); nuclei were detected by counter staining with DAPI (blue). (C, D) Quantitative analysis of intensities of PTH and CHGA immunofluorescence normalized to nuclear fluorescence. Data are shown for the surface (A, C) and the cross-sectional center (B, D) of each spheroid group. Scale bars: 50 μm. Data were analyzed using one-way ANOVA and are expressed as means ± S.D. (n = 15). Different letters indicate significant differences among experimental groups ($P < 0.05$). (For interpretation of the references to color in this figure legend, the reader is referred to the web version of this article.)

survival rates significantly dropped shortly after implantation. For PTX-SP1 rats, the survival rate for the first 40 days after implantation was 40% and further dropped to 20% at the end of the experiment. Body weights in both sham and PTX-SP2 groups increased throughout the experiment; PTX-SP2 rats exhibited a modest weight gain (135.1% ± 58.4%) over 3 months, where weight gain in sham-operated rats was 159.3% ± 9.5%. No clear gain in weight was observed in PTX-SP1 rats (118.76% ± 47.8%) (Fig. 5B).

3.5. Restoration of iPTH and iCa^{2+} levels in PTX rats implanted with dTMSC spheroids

Serum iPTH concentrations in sham rats fed normal and calcium-free diets were 64.4–86.9 pg/mL and 34.0–155.1 pg/mL, respectively, throughout the experimental period (Fig. 6A and B). However, the iPTH concentration in PTX-PBS rats was 62.0 ± 11.7 pg/mL at day 0, and then significantly decreased to 13.9 ± 2.1 pg/mL at day 7

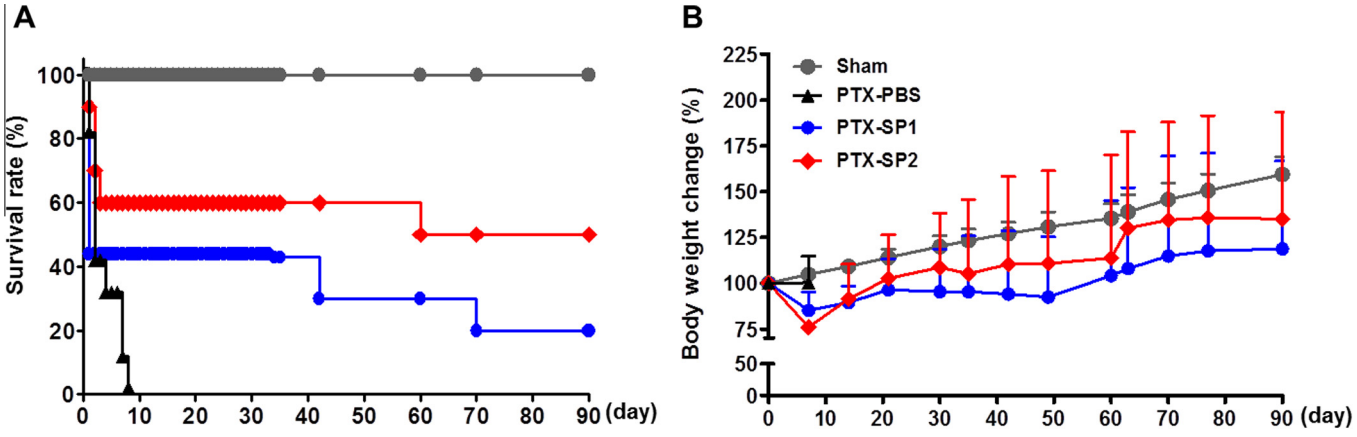

Fig. 5. Survival rates and body weight changes over 3 months in PTX rats implanted with TMSC spheroids. The *in vivo* therapeutic efficacy of differentiated TMSC spheroids was examined using PTX rats. (A) Survival rates of the different experimental animal groups. The survival rate of the sham group was used as a reference. SP1 and SP2, used for control and differentiated TMSC spheroids, respectively, were subcutaneously implanted into PTX rats (PTX-SP1 and PTX-SP2 groups, respectively). PBS (PTX-PBS) were used a negative control~~s~~, respectively. (B) Changes in body weight were measured in each animal group.

Please cite this article in press as: Y.S. Park et al., Scaffold-free parathyroid tissue engineering using tonsil-derived mesenchymal stem cells, Acta Biomater. (2016), http://dx.doi.org/10.1016/j.actbio.2016.03.003

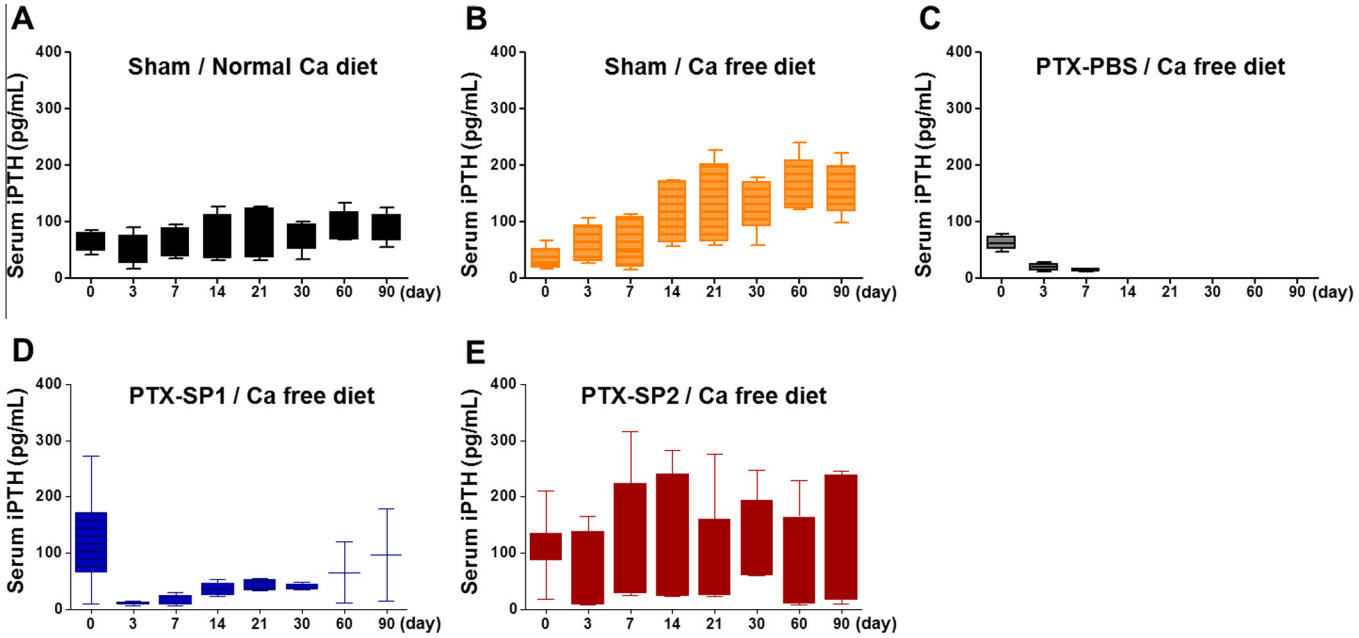

Fig. 6. Serum iPTH concentrations in PTX rats implanted with TMSC spheroids. Sham rats fed a normal (A) or calcium-free (B) diet showed serum iPTH concentrations in the normal physiological range, although levels were higher in sham rats fed a calcium-free diet. (C) Serum iPTH concentration acutely decreased in PTX-PBS rats, as reported previously. (D) In PTX-SP1 rats, serum iPTH was below physiological levels (10.8–39.1 pg/mL) until day 30. Only two rats survived at 2 and 3 months, and showed large differences in PTH level between them. (E) PTX-SP2 rats maintained their iPTH levels within the physiological range (57.7–128.2 pg/mL) for 3 months.

(Fig. 6C). Similar to survival rates, serum iPTH levels in PTX-SP1 rats significantly decreased from 120.6 ± 79.0 pg/mL to negligible levels (10.8 ± 3.5 pg/mL) after day 3 (Fig. 6D). Although this decreased iPTH level slightly rebounded (to 39.1 ± 6.2 pg/mL) by 1 month, it was still significantly lower than physiological levels of iPTH [22]. At this point, it should be noted that iPTH values in PTX-SP1 rats reported for 2 and 3 months are not reliable because only two surviving rats were available for assays and their iPTH levels were widely divergent. In contrast, PTX-SP2 rats showed a considerable amount of serum iPTH even after day 3 (57.7 ± 17.8 pg/mL); serum iPTH was maintained at a relatively stable plateau level throughout the experimental period (57.7–128.2 pg/mL), concentrations that were within the normal physiological range or even slightly elevated (Fig. 6E).

We next examined serum levels of iCa^{2+} among experimental groups because of the key role of iCa^{2+} in calcium homeostasis in human physiology. As expected, iCa^{2+} concentrations in sham rats were normal (1.15–1.20 mmol/L) throughout the experiment (Fig. 7). However, the iCa^{2+} concentration in PTX-PBS rats decreased abruptly to 0.35 ± 0.01 mmol/L at day 10, a drop that might have been responsible for the death of all rats in this group. The levels of iCa^{2+} in PTX-SP1 rats were similar to those in PTX-PBS rats throughout the experimental period and were significantly lower than normal. In contrast, iCa^{2+} levels in PTX-SP2 rats were considerably higher and stable throughout the experimental period; at day 90, they reached at least 0.70 ± 0.11 mmol/L, which is at the low end of the normal physiological range.

3.6. Assessment of implanted TMSC spheroids in PTX rats

We evaluated the fate of implanted TMSC spheroids in PTX rats. Using intraperitoneal injection of 5-ALA as a photosensitizing strategy, we found distinct red fluorescent spots in the skin area of implanted spheroids in rats, suggesting the presence of live parathyroid-like cells. Compared with the PTX-SP1 group, which exhibited only a few (Fig. 8A, arrows) or virtually no (Fig. 8B) red fluorescent spots, PTX-SP2 rats showed abundant red spots in isolated skin tissues of the implanted area (Fig. 8C, arrows in white dotted box). Because there were so few red spots in PTX-SP1 rats, only skin tissue isolated from PTX-SP2 rats was prepared as a paraffin-embedded sample and sectioned for further immunofluorescence assays. A microscopic image of sectioned skin tissue detected implanted SP2 (Fig. 8D, arrows).

We also detected more vascularization in the PTX-SP2 than in the PTX-SP1 group (Fig. 8A and C, yellow arrowheads). The blood vessel formation in skin tissue isolated from PTX-SP2 rats was clearly confirmed by the immunofluorescence assay using anti-CD31 antibody (Fig. 8E); microvessels of ~180 μm in diameter were detected.

We next examined whether implanted TMSC spheroids (Fig. 8F, arrows) express PTH and CHGA in isolated implanted skin areas. As shown in Fig. 8F, PTH and CHGA expression were significantly higher in the implant area of PTX-SP2 rats. We also found a hollow space in the implanted spheroids (Fig. 8F, an asterisk). Finally, the parathyroid-like tissue regeneration was further confirmed by the identification of GCM2 protein expression in the implant area of PTX-SP2 rats (Fig. 8G). GCM2 is another parathyroid tissue-specific marker protein.

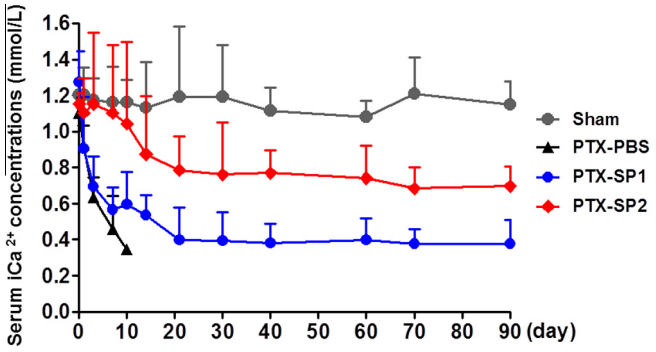

Fig. 7. Serum iCa^{2+} levels in PTX rats implanted with TMSC spheroids. Sham rats maintained steady physiological levels of iCa^{2+} (1.15 ± 0.13 mmol/L) throughout the experimental period. PTX-PBS rats showed a rapid decrease in iCa^{2+} levels (0.35 ± 0.01 mmol/L) at day 10. Similarly, PTX-SP1 rats also showed a rapid drop in iCa^{2+} levels in 10 days, which thereafter gradually decreased to 0.38 mmol/L, a value considered below physiological levels and possibly capable of inducing tetany. In contrast, PTX-SP2 rats showed iCa^{2+} levels (1.10–0.70 mmol/L), close to the lower end of the physiological range, throughout the experimental period.

Please cite this article in press as: Y.S. Park et al., Scaffold-free parathyroid tissue engineering using tonsil-derived mesenchymal stem cells, Acta Biomater. (2016), http://dx.doi.org/10.1016/j.actbio.2016.03.003

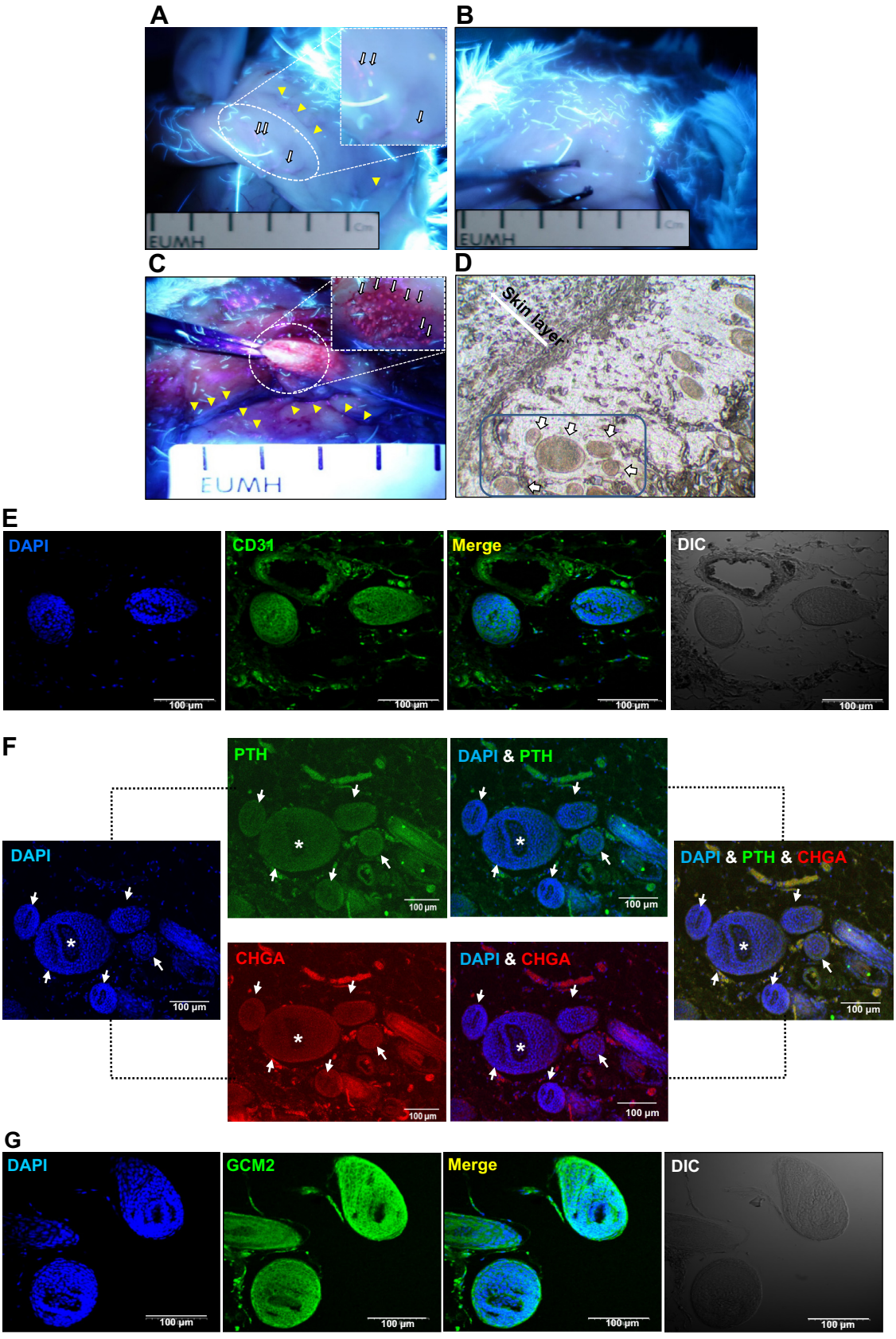

Fig. 8. Detection of regenerated parathyroid-like tissue in PTX-SP2 rats. Three months after implantation, TMSC spheroids, SP1 (A and B) and SP2 (C and D), were identified in the isolated skin tissues of PTX rats. Parathyroid-like tissue stained by 5-ALA was detected as a red color, indicated by an arrow (A, C) and white dotted circle (C). The number of implanted TMSC spheroids and associated degree of vascularization in the implantation area were significantly greater in PTX-SP2 than in PTX-SP1 rats. (D) Paraffin-embedded section of the isolated skin area from PTX-SP2 rats. (E) Blood vessel formation in SP2 implanted area was clearly detected by the immunofluorescence assay using anti-CD31 antibody. (F) Immunofluorescence confirmed the presence of PTH and CHGA expression in implanted SP2 spheroids. (G) In addition to PTH and CHGA, the implanted SP2 spheroids also significantly expressed GCM2, another parathyroid cell-specific protein. (For interpretation of the references to color in this figure legend, the reader is referred to the web version of this article.)

Please cite this article in press as: Y.S. Park et al., Scaffold-free parathyroid tissue engineering using tonsil-derived mesenchymal stem cells, Acta Biomater. (2016), http://dx.doi.org/10.1016/j.actbio.2016.03.003

3.7. In vitro and in vivo expression of N-cadherin in dTMSC spheroids

We further examined the expression of cell adhesion factors that enhance TMSC spheroid survival and biocompatibility during implantation in rats. To this end, we focused on N-cadherin, which has previously been reported to serve as an indicator of cell-cell interactions that accelerate osteogenic potential in human AD-MSC [23]. As shown in Fig. 9, an immunofluorescence assay revealed higher levels of N-cadherin expression in SP2 (Fig. 9B) than in SP1 (Fig. 9A). An *in vitro* analysis of SP1 and SP2 also detected a hollow space inside each spheroid (Fig. 9A and B, an asterisk). Furthermore, N-cadherin was mainly expressed on the surface of SP2 spheroids, where it is presumably involved in the engraftment of spheroids in the body [24]. These data were also confirmed by a Western blot analysis using an N-cadherin specific antibody, which showed higher (2.4 ± 0.4-fold) N-cadherin expression in SP2 compared with SP1 (Fig. 9C). Similar to *in vitro* data, we also found significantly higher levels of N-cadherin expression in PTX-SP2 rat skin areas, most of which appeared at the outer margin of spheroids (Fig. 9D).

4. Discussion

We recently reported that dTMSC restore *in vivo* parathyroid cell functions in PTX rats fed a calcium-free diet, but only if embedded in Matrigel, a commercially-available biomaterial scaffold [8].

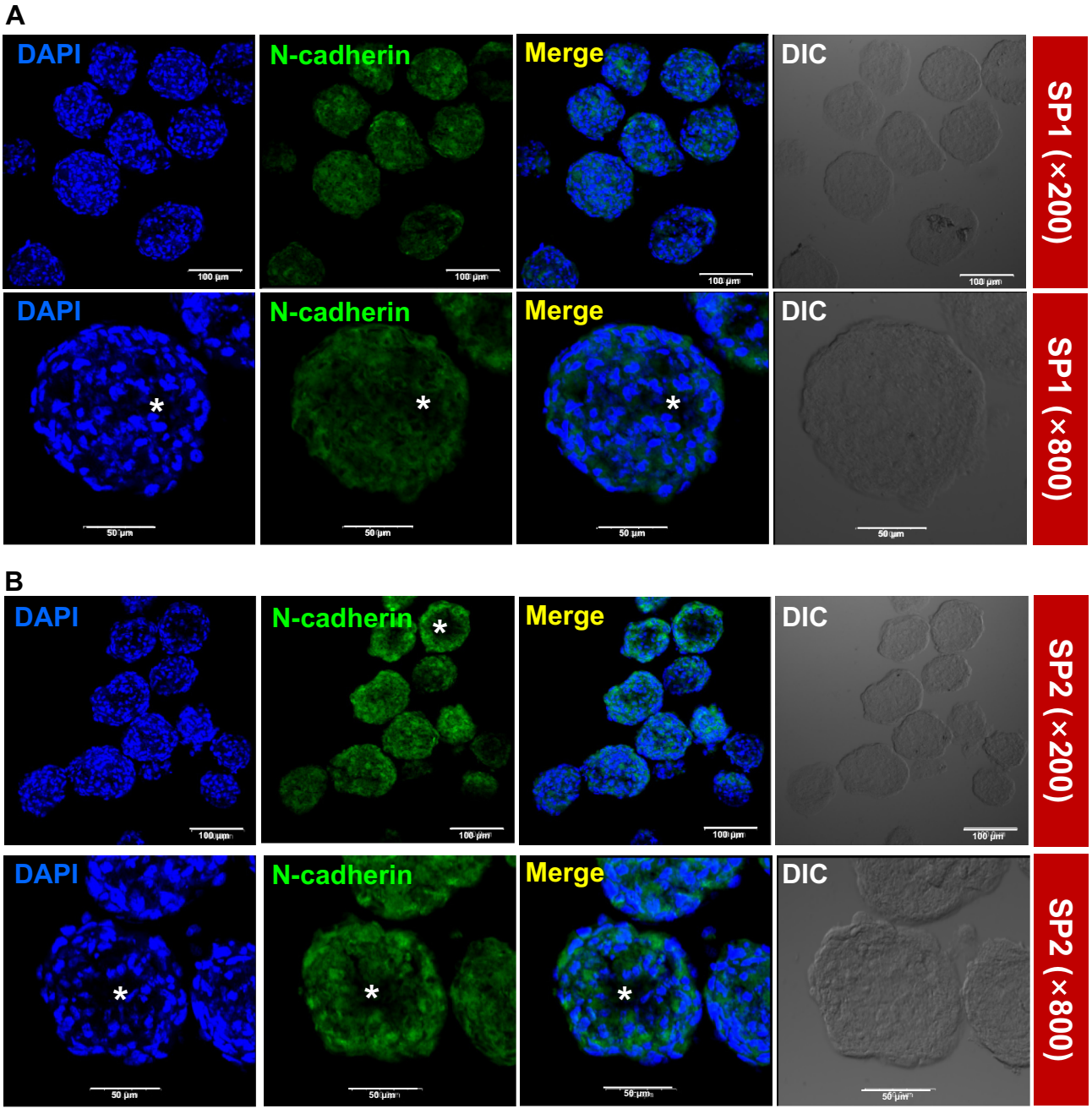

Fig. 9. Expression of N-cadherin in TMSC spheroids. (A, B) Immunofluorescence confocal microscopy revealed significant *in vitro* expression of N-cadherin protein in SP2; SP1 also expressed N-cadherin, albeit to a much lesser extent. Scale bar: 100 μm (top) and 50 μm (bottom). (C) Significant N-cadherin protein expression in SP2 was also confirmed using a Western blot analysis. GAPDH protein was used as an internal standard ($P < 0.05$). (D) Significant N-cadherin expression was detected in SP2-implanted skin tissue.

Please cite this article in press as: Y.S. Park et al., Scaffold-free parathyroid tissue engineering using tonsil-derived mesenchymal stem cells, Acta Biomater. (2016), http://dx.doi.org/10.1016/j.actbio.2016.03.003

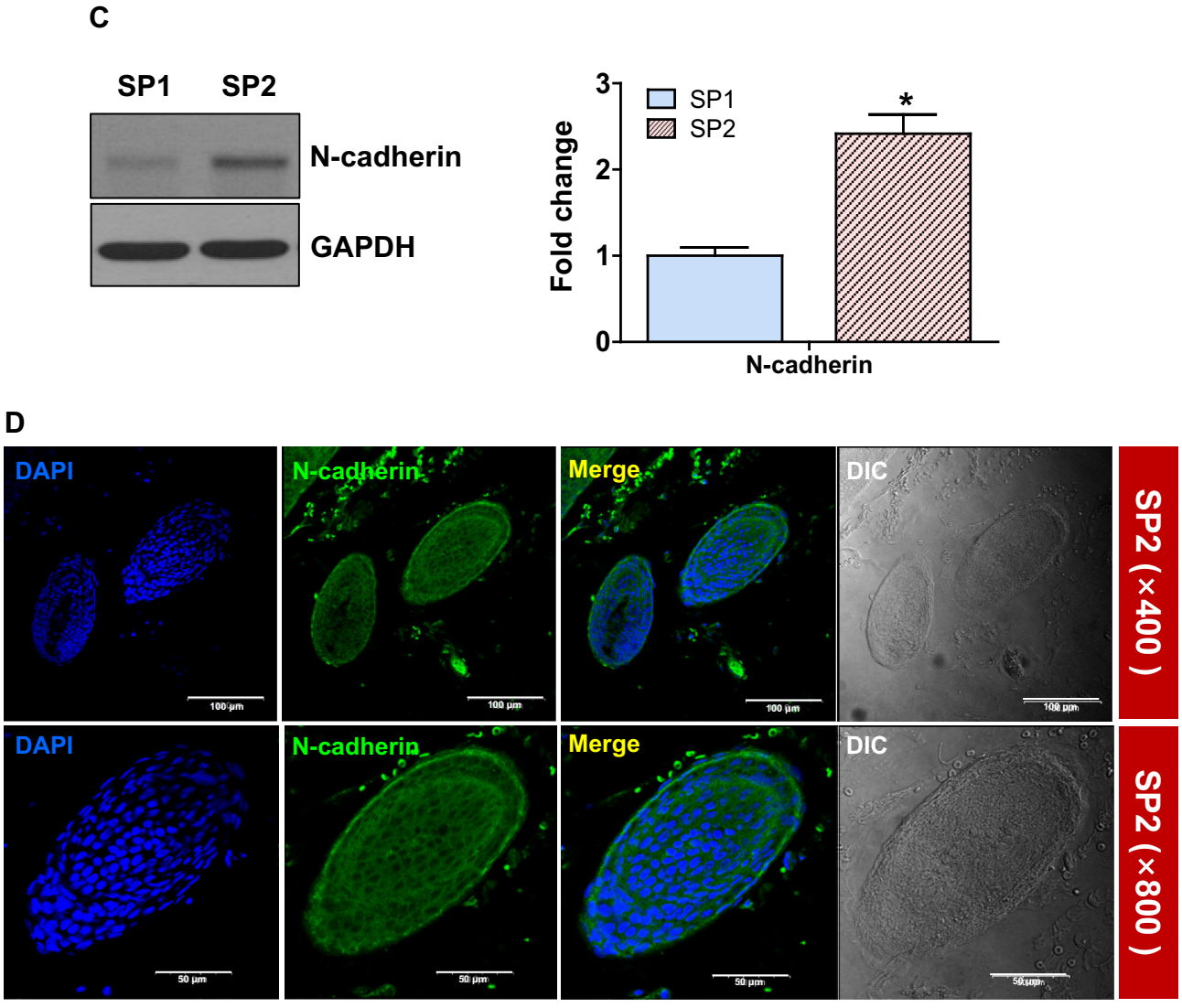

Fig. 9 (*continued*)

Although biomaterial scaffolds provide the structural support for cell attachment, thus possibly increasing the viability of implanted cells under *in vivo* conditions, they are still associated with several drawbacks. These include difficulties of loaded cells migrating into the scaffolds (penetration of cells), insufficient oxygen supply for the loaded cells [25], non-uniform growth of cells inside scaffolds, and inappropriate mechano-physical characteristics for tissue applications [26,27]. To overcome limitations associated with the use of scaffolds, researchers have developed 3D spheroidal culture technology using target cells alone [28–31]. In the current study, we examined whether a scaffold-free, spheroidal architecture of TMSC alone restores *in vivo* parathyroid cell functions in a PTX rat model. Our results clearly demonstrated that implantation with dTMSC spheroids alone, without biomaterial scaffolds, significantly increases survival rates and restores the levels of iPTH and iCa^{2+} in PTX rats throughout an extended experimental period (3 months). These results may open a new paradigm for parathyroid regeneration that could ultimately evolve into an improved clinical application.

Compared with the ~10 weeks required for transdifferentiation of thymic epithelial cells into cells that release PTH [7], we recently reported that 7 days are sufficient for TMSC to differentiate into PTH-releasing parathyroid cells [8]. Here, we also demonstrated that only a 7-day differentiation period in 3D culture plates is sufficient for TMSC to differentiate into cells expressing PTH and CHGA; longer exposures to differentiation condition (14 days) in 3D plates significantly decreased TMSC viability, suggesting that chemicals used for differentiation may adversely affect cell viability. In this regard, differentiation is known to be inversely proportional to proliferation [32]. Why a shorter exposure is better is not yet clear, but it may indicate that an appropriate time is required for TMSC to aggregate and form a spheroidal structure before differentiating into parathyroid cells. Whether the differentiation medium itself inhibits spheroidal formation will require further investigation. Nonetheless, our study suggests that minimizing the *in vitro* differentiation time to the most possible extent may maximize the *in vivo* bioactivity of spheroidal cells, from a functional and/or economic standpoint.

In addition to significantly higher levels of PTH and CHGA expression in dTMSC spheroids (SP2) compared with cTMSC spheroids (SP1), the levels of N-cadherin expression in the former were also significantly higher. Because of the role of N-cadherin in cell-cell and cell-tissue interactions [33], higher expression of N-cadherin might be expected to increase the implantation efficacy of spheroids. This expectation is reflected in the greater number of implanted TMSC spheroids observed in PTX-SP2 rats compared

Please cite this article in press as: Y.S. Park et al., Scaffold-free parathyroid tissue engineering using tonsil-derived mesenchymal stem cells, Acta Biomater. (2016), http://dx.doi.org/10.1016/j.actbio.2016.03.003

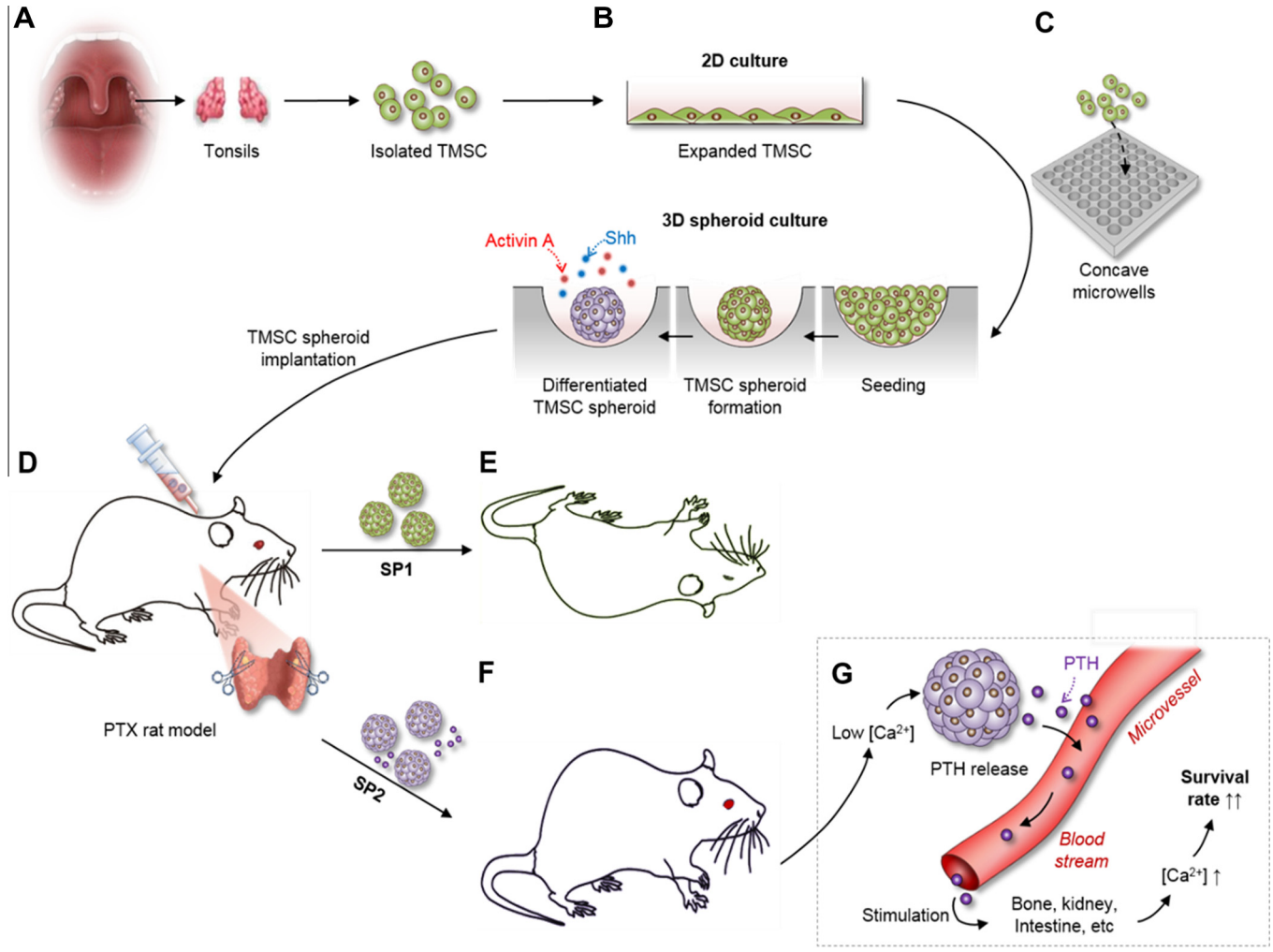

Fig. 10. Schematic representation of parathyroid regeneration by scaffold-free differentiated TMSC spheroids. (A) TMSCs are isolated from tonsillar tissues, (B) expanded on a 2D culture system, and (C) then seeded on PDMS-based concave microwell molds to construct 3D spheroids. TMSC are differentiated using differentiation culture medium containing activin A and sonic hedgehog (Shh) under the indicated experimental conditions, producing a differentiated TMSC spheroid (SP2). Control spheroids (SP1) are prepared by culturing without differentiation. (D) PTX rats were established, fed a calcium-free diet, and subcutaneously implanted with SP1 (PTX-SP1) or SP2 (PTX-SP2). (E) Over 3 months after implantation, PTX-SP1 rats showed 20% survival rates with low levels of serum iPTH and iCa^{2+}. (F) Half of all PTX-SP2 rats survived, with physiological levels of serum iPTH and iCa^{2+}. (G) Better survival rates in PTX-SP2 are likely explained by SP2 implanted in PTX-SP2 rats releasing a physiological level of iPTH, which controls Ca^{2+} homeostasis in the body. Newly formed microvessels, perhaps induced by SP2, may support iPTH actions on target tissues by aiding its systematic circulation.

with the very few in rats implanted with SP1 (Fig. 8). Whether N-cadherin is directly involved in implantation efficacy in our system needs further investigation, for example using knockdown approaches. In contrast, we found little expression of another important attachment protein, E-cadherin, in TMSC regardless of differentiation status, indicating that E-cadherin is not likely involved in mediating cell-cell or cell-tissue attachment under our experimental conditions. It was previously reported that hESC express E-cadherin, which is involved in increasing spheroidal formation through inhibition of Wnt signaling [34]. E-cadherin is known to be of epithelial origin, whereas N-cadherin is of mesodermal origin [35]. In this context, TMSC are likely to be mixed cells originating from both endoderm and mesoderm [30,36]. We also detected much more vascularization around implanted dTMSC spheroids than cTMSC spheroids in PTX rats, a finding that reproduces the greater vascularization observed in PTX rats implanted with Matrigel-embedded dTMSC compared to those with cTMSC [8]. These results clearly demonstrate that differentiation induces vessel formation in an *in vivo* system, thereby increasing survival rates.

Immunofluorescence assays also clearly revealed a hollow structure in TMSC spheroids (Figs. 8E and 9, an asterisk), suggesting that cells are not closely packed in the spheroids. At present, we do not fully understand how our 3D culture condition forms the hollow structure. Previously, it was reported that spheroids having a size greater than ~150 μm in diameter may develop a necrotic core due to a limited diffusion of oxygen [37]; the sizes of our TMSC spheroids under our condition were greater than ~150 μm until day 5 (Fig. 2C). Nonetheless, it is likely that the hollow structure has its own advantage; it can let blood microvessels penetrate into centers of spheroids, helping oxygen and/or nutrient supply in *in vivo* system. Confirmation of this supposition awaits a further investigation of the detailed underlying mechanism.

Under our conditions, the survival rates of PTX rats implanted with TMSC spheroids decreased rapidly within 1–2 days of implantation before subsequently stabilizing. Although a previous study showed that the use of Matrigel-embedded TMSC enhanced survival rates somewhat longer (3–4 days), the difference between the two experimental conditions is unlikely statistically significant.

Please cite this article in press as: Y.S. Park et al., Scaffold-free parathyroid tissue engineering using tonsil-derived mesenchymal stem cells, Acta Biomater. (2016), http://dx.doi.org/10.1016/j.actbio.2016.03.003

It is presently unclear why the survival rates in PTX rats implanted with TMSC spheroids decreased rapidly. One possibility is that an adhesion factor such as N-cadherin improves the early engraftment of implanted spheroids, increasing TMSC viability in spheroids [23], although this remains to be demonstrated. However, after their initial rapid decrease in survival rate, PTX rats implanted with TMSC spheroids maintained relative stability for an extended period (40–60 days), indicating that controlling survival rates in as few as 3–4 days after PTX could determine the success of *in vivo* parathyroid regeneration under our conditions.

We previously reported that serum iPTH levels in PTX rats implanted with Matrigel-embedded TMSC increase continuously during the experimental period (up to 1 month) [8]. Although a direct comparison is not possible, the use of scaffold-free TMSC spheroids restored iPTH to more physiological levels and more persistently (3 months) than the use of Matrigel-embedded TMSC. Thus, at minimum, dTMSC spheroids themselves are likely to have a better capacity to control *in vivo* serum iPTH levels than scaffolded TMSC, although the mechanism underlying this improvement is not yet defined.

5. Conclusion

Although our previous study proposed the requirement of scaffold(s) for parathyroid cells to exert their *in vivo* functions in PTX rats fed a calcium-free diet, the current study is the first report that the implantation with dTMSC spheroids alone, without any biomaterial scaffolds, significantly increases survival rates and restores the levels of iPTH and iCa^{2+} in PTX rats throughout an more extended experimental period (3 months) (Fig. 10). This new strategy may open a new paradigm for parathyroid regeneration that could ultimately evolve into an improved clinical application. Lastly, TMSC spheroids may also provide a convenient and efficient scaffold-free platform for researchers investigating conditions involving abnormal calcium homeostasis, such as osteoporosis.

Acknowledgements

This study was supported in part by the Basic Science Research Program through the National Research Foundation of Korea (NRF) funded by the Ministry of Science, ICT & Future Planning (NRF-2012M3A9C6049728, NRF-2013R1A1A3007591, and NRF-2015R1A2A1A09004998), and by a grant of the Korea Health Technology R&D Project through the Korea Health Industry Development Institute (KHIDI), funded by the Ministry of Health & Welfare, Republic of Korea (grant number: HI14C-1557-020014) and also this work was supported in part by RP-Grant 2015 of Ewha Womans University.

References

[1] J.P. Bilezikian, A.A. Khan, J.T. Potts Jr., Third International Workshop on the Management of Asymptomatic Primary Hyperthyroidism, Guidelines for the management of asymptomatic primary hyperparathyroidism: summary statement from the third international workshop, J. Clin. Endocrinol. Metab. 94 (2009) 335–339.
[2] J.P. Bilezikian, A. Khan, J.T. Potts Jr., M.L. Brandi, B.L. Clarke, D. Shoback, H. Juppner, P. D'Amour, J. Fox, L. Rejnmark, L. Mosekilde, M.R. Rubin, D. Dempster, R. Gafni, M.T. Collins, J. Sliney, J. Sanders, Hypoparathyroidism in the adult: epidemiology, diagnosis, pathophysiology, target-organ involvement, treatment, and challenges for future research, J. Bone Miner. Res. 26 (2011) 2317–2337.
[3] C. Bieglmayer, G. Prager, B. Niederle, Kinetic analyses of parathyroid hormone clearance as measured by three rapid immunoassays during parathyroidectomy, Clin. Chem. 48 (2002) 1731–1738.
[4] G.H. Sakorafas, V. Stafyla, C. Bramis, N. Kotsifopoulos, T. Kolettis, G. Kassaras, Incidental parathyroidectomy during thyroid surgery: an underappreciated complication of thyroidectomy, World J. Surg. 29 (2005) 1539–1543.
[5] J. Wang, L. Liao, S. Wang, J. Tan, Cell therapy with autologous mesenchymal stem cells-how the disease process impacts clinical considerations, Cytotherapy 15 (2013) 893–904.
[6] A.I. Caplan, Review: mesenchymal stem cells: cell-based reconstructive therapy in orthopedics, Tissue Eng. 11 (2005) 1198–1211.
[7] K.M.W. Ignatoski, E.L. Bingham, L.K. Frome, G.M. Doherty, Directed transdifferentiation of thymus cells into parathyroid-like cells without genetic manipulation, Tissue Eng. Part C Methods. 17 (2011) 1051–1059.
[8] Y.S. Park, H.S. Kim, Y.M. Jin, Y. Yu, H.Y. Kim, H.S. Park, S.C. Jung, K.H. Han, Y.J. Park, K.H. Ryu, I. Jo, Differentiated tonsil-derived mesenchymal stem cells embedded in Matrigel restore parathyroid cell functions in rats with parathyroidectomy, Biomaterials 65 (2015) 140–152.
[9] G.D. DuRaine, W.E. Brown, J.C. Hu, K.A. Athanasiou, Emergence of scaffold-free approaches for tissue engineering musculoskeletal cartilages, Ann. Biomed. Eng. 43 (2015) 543–554.
[10] A. Akkouch, Y. Yu, I.T. Ozbolat, Microfabrication of scaffold-free tissue strands for three-dimensional tissue engineering, Biofabrication 7 (2015) 031002.
[11] S.F. Wong, Y. No da, Y.Y. Choi, D.S. Kim, B.G. Chung, S.H. Lee, Concave microwell based size-controllable hepatosphere as a three-dimensional liver tissue model, Biomaterials 32 (2011) 8087–8096.
[12] D. Yoon No, K.H. Lee, J. Lee, S.H. Lee, 3D liver models on a microplatform: well-defined culture, engineering of liver tissue and liver-on-a-chip, Lab Chip 15 (2015) 3822–3837.
[13] Y. No da, S.A. Lee, Y.Y. Choi, D. Park, J.Y. Jang, D.S. Kim, S.H. Lee, Functional 3D human primary hepatocyte spheroids made by co-culturing hepatocytes from partial hepatectomy specimens and human adipose-derived stem cells, PLoS One 7 (2012) e50723.
[14] Y. No da, G.S. Jeong, S.H. Lee, Immune-protected xenogeneic bioartificial livers with liver-specific microarchitecture and hydrogel-encapsulated cells, Biomaterials 35 (2014) 8983–8991.
[15] Y. Jun, A.R. Kang, J.S. Lee, G.S. Jeong, J. Ju, D.Y. Lee, S.H. Lee, 3D co-culturing model of primary pancreatic islets and hepatocytes in hybrid spheroid to overcome pancreatic cell shortage, Biomaterials 34 (2013) 3784–3794.
[16] Y. Jun, A.R. Kang, J.S. Lee, S.J. Park, D.Y. Lee, S.H. Moon, S.H. Lee, Microchip-based engineering of super-pancreatic islets supported by adipose-derived stem cells, Biomaterials 35 (2014) 4815–4826.
[17] K.H. Ryu, K.A. Cho, H.S. Park, J.Y. Kim, S.Y. Woo, I. Jo, Y.H. Choi, Y.M. Park, S.C. Jung, S.M. Chung, B.O. Choi, H.S. Kim, Tonsil-derived mesenchymal stromal cells: evaluation of biologic, immunologic and genetic factors for successful banking, Cytotherapy 14 (2012) 1193–1202.
[18] E.L. Bingham, S.P. Cheng, K.M. Woods Ignatoski, G.M. Doherty, Differentiation of human embryonic stem cells to a parathyroid-like phenotype, Stem Cells Dev. 18 (2009) 1071–1080.
[19] Y.Y. Choi, B.G. Chung, D.H. Lee, A. Khademhosseini, J.H. Kim, S.H. Lee, Controlled-size embryoid body formation in concave microwell arrays, Biomaterials 31 (2010) 4296–4303.
[20] J.Y. Park, D.H. Lee, E.J. Lee, S.H. Lee, Study of cellular behaviors on concave and convex microstructures fabricated from elastic PDMS membranes, Lab Chip 9 (2009) 2043–2049.
[21] H.S. Park, S.Y. Jung, H.Y. Kim, Y. Kim da, M.S. Kim, S.M. Chung, Y.S. Rho, H.S. Kim, Development of hypoparathyroidism animal model and the feasibility of small intestinal submucosa application on the parathyroid autotransplantation, Eur. Arch. Otorhinolaryngol. 272 (2015) 2969–2977.
[22] L. Youngwirth, J. Benavidez, R. Sippel, H. Chen, Parathyroid hormone deficiency after total thyroidectomy: incidence and time, J. Surg. Res. 163 (2010) 69–71.
[23] S.H. Hsu, Y.H. Ni, Y.C. Lee, Microwell chips for selection of bio-macromolecules that increase the differentiation capacities of mesenchymal stem cells, Macromol. Biosci. 13 (2013) 1100–1109.
[24] K. Hosokawa, F. Arai, H. Yoshihara, H. Iwasaki, Y. Nakamura, Y. Gomei, T. Suda, Knockdown of N-cadherin suppresses the long-term engraftment of hematopoietic stem cells, Blood 116 (2010) 554–563.
[25] T. Billiet, M. Vandenhaute, J. Schelfhout, S. Van Vlierberghe, P. Dubruel, A review of trends and limitations in hydrogel-rapid prototyping for tissue engineering, Biomaterials 33 (2012) 6020–6041.
[26] J.C. Dunn, W.Y. Chan, V. Cristini, J.S. Kim, J. Lowengrub, S. Singh, B.M. Wu, Analysis of cell growth in three-dimensional scaffolds, Tissue Eng. 12 (2006) 705–716.
[27] M. Frydrych, S. Roman, S. MacNeil, B. Chen, Biomimetic poly(glycerol sebacate)/poly(l-lactic acid) blend scaffolds for adipose tissue engineering, Acta Biomater. 18 (2015) 40–49.
[28] S.E. Yeon, Y. No da, S.H. Lee, S.W. Nam, I.H. Oh, J. Lee, H.J. Kuh, Application of concave microwells to pancreatic tumor spheroids enabling anticancer drug evaluation in a clinically relevant drug resistance model, PLoS ONE 8 (2013) e73345.
[29] H.H. Yoon, S.H. Bhang, J.Y. Shin, J. Shin, B.S. Kim, Enhanced cartilage formation via three-dimensional cell engineering of human adipose-derived stem cells, Tissue Eng. Part A 18 (2012) 1949–1956.
[30] J.K. Hong, J. Yun, H. Kim, S.M. Kwon, Three-dimensional culture of mesenchymal stem cells, Tissue Eng. Regen. Med. 12 (2015) 211–221.
[31] S. Breslin, L. O'Driscoll, Three-dimensional cell culture: the missing link in drug discovery, Drug Discov. Today 18 (2013) 240–249.
[32] Z. Grossman, The stem-cell concept revisited - self-renewal capacity is a dynamic property of hematopoietic-cells, Leuk. Res. 10 (1986) 937–950.

Please cite this article in press as: Y.S. Park et al., Scaffold-free parathyroid tissue engineering using tonsil-derived mesenchymal stem cells, Acta Biomater. (2016), http://dx.doi.org/10.1016/j.actbio.2016.03.003

[33] E. Fennema, N. Rivron, J. Rouwkema, C. van Blitterswijk, J. de Boer, Spheroid culture as a tool for creating 3D complex tissues, Trends Biotechnol. 31 (2013) 108–115.
[34] E.J. Lee, S.J. Park, S.K. Kang, G.H. Kim, H.J. Kang, S.W. Lee, H.B. Jeon, H.S. Kim, Spherical bullet formation via E-cadherin promotes therapeutic potency of mesenchymal stem cells derived from human umbilical cord blood for myocardial infarction, Mol. Ther. 20 (2012) 1424–1433.
[35] A. Peralta Soler, K.A. Knudsen, A. Tecson-Miguel, F.X. McBrearty, A.C. Han, H. Salazar, Expression of E-cadherin and N-cadherin in surface epithelial-stromal tumors of the ovary distinguishes mucinous from serous and endometrioid tumors, Hum. Pathol. 28 (1997) 734–739.
[36] E.S. Kim, G.M. Keating, Recombinant human parathyroid hormone (1–84): A review in hypoparathyroidism, Drugs 75 (2015) 1293–1303.
[37] Y.C. Tung, A.Y. Hsiao, S.G. Allen, Y.S. Torisawa, M. Ho, S. Takayama, High-throughput 3D spheroid culture and drug testing using a 384 hanging drop array, Analyst 136 (2011) 473–478.

Please cite this article in press as: Y.S. Park et al., Scaffold-free parathyroid tissue engineering using tonsil-derived mesenchymal stem cells, Acta Biomater. (2016), http://dx.doi.org/10.1016/j.actbio.2016.03.003